Aquaculture Reports 38 (2024) 102317

Contents lists available at ScienceDirect

Aquaculture Reports

journal homepage: www.elsevier.com/locate/aqrep

Zinc oxide nanoparticles cause hepatotoxicity in rare minnow (*Gobiocypris rarus*) via ROS-mediated oxidative stress and apoptosis activation and inhibition of lipid peroxidation

Liangxia Su [a,1], Huanhuan Li [a,1], Jiahuan Wang [a], Jinming Wu [b], Jing Wan [a], Yongfeng He [c], Jun Liu [a,*]

[a] *Hubei Key Laboratory of Animal Nutrition and Feed Science, Engineering Research Center of Feed Protein Resources on Agricultural By-Products, Ministry of Education, Wuhan Polytechnic University, Wuhan, China*

[b] *Key Laboratory of Freshwater Biodiversity Conservation, Ministry of Agriculture and Rural Affairs of China, Yangtze River Fisheries Research Institute, Chinese Academy of Fishery Sciences, Wuhan 430223, China*

[c] *The Key Laboratory of Aquatic Biodiversity and Conservation of Chinese Academy of Sciences, Institute of Hydrobiology, Chinese Academy of Sciences, Wuhan, Hubei, China*

ARTICLE INFO

Keywords:
Zinc oxide nanoparticle
Liver injuries
Gobiocypris rarus
ROS-mediated oxidative stress and apoptosis
Lipid metabolism

ABSTRACT

Zinc oxide nanoparticles (ZnO NPs) measuring 30 ± 10 nm in diameter are utilized in various applications, including batteries, plastics, ceramics, cosmetics, flame retardants, and food. However, their potential impact and risk on aquatic ecosystems remain unclear. This study examined the hepatotoxic effects of dietary ZnO NPs in rare minnow. Three hundred rare minnows were fed diets containing 0 mg/kg, 20 mg/kg and 60 mg/kg of ZnO NPs for 60 days, with hepatotoxicity assessments at 15-day intervals. The histological data showed that ZnO NPs severely damage liver tissues, causing cytoplasmic vacuolization and irregular or missing nuclei. The treatment groups showed a significant rise in the liver injury index ($P < 0.05$). Moreover, there was a notable increase in zinc accumulation in the ZnO NPs groups compared to the control group ($P < 0.05$). ZnO NPs also reduced body weight and hepato-somatic index (HSI) in rare minnows. The enzyme activity results showed elevated levels of reactive oxygen species (ROS), total cholesterol (T-CHO), triglyceride (TG), acetyl Coa carboxylase (ACC), and fatty acid synthase (FAS) in the ZnO NPs fed groups, while total antioxidant capacity (T-AOC) and malondialdehyde (MDA) decreased. Further investigation found that accumulation of ZnO NPs in the liver tissues up-regulated the levels of genes related to antioxidant (*mn-sod*, *cat* and *nf-κb*), pro-apoptotic (*bax*) and lipogenesis (*gpat3*, *dgat1a* and *dgat1b*), while down-regulating genes associated with lipid catabolism (*cpt1* and *tpi1*). These findings suggest that dietary ZnO NPs cause hepatotoxicity by inducing oxidative stress through ROS, triggering apoptosis, and inhibiting lipid peroxidation. The results indicate that ZnO NPs may pose a significant threat to aquatic animals and ecosystems.

1. Introduction

Nanoparticles (NPs) have become ubiquitous daily due to their extensive use in healthcare, industry, and household products (Fonseca et al., 2023; Gad et al., 2021; Stoller and Ochando-Pulido, 2020). Zinc oxide nanoparticles (ZnO NPs), known for their absorption, antimicrobial, antioxidant, immunomodulatory, and growth-promoting properties, have recently been used as feed additives to enhance breeding quality. Studies have demonstrated that ZnO NPs can improve growth performance, health status, and stress resistance in fish species such as rabbitfish (*Siganus rivulatus*) (Sallam et al., 2020), grass carp (*Ctenopharyngodon idella*) (Faiz et al., 2015), gilthead seabream (*Sparus aurata*) (Izquierdo et al., 2017) and nile tilapia (*Oreochromis niloticus*) (Mohammady et al., 2021). However, the potential toxicity and mechanisms of ZnO NPs as dietary supplements remain unclear.

The widespread production and use of ZnO NPs inevitably lead to their release into the environment. Research has shown that water-phase ZnO NPs induce nephrotoxic (Alkaladi et al., 2015), immunotoxic (Choi

* Corresponding author.
E-mail address: 673164434@qq.com (J. Liu).
[1] These authors have contributed equally to this work.

https://doi.org/10.1016/j.aqrep.2024.102317
Received 19 April 2024; Received in revised form 18 August 2024; Accepted 19 August 2024
Available online 27 August 2024

et al., 2016), and hepatotoxic (Rajkumar et al., 2022) effects in aquatic organisms. The liver and kidneys are the main targets for ZnO NPs accumulation, and food-phase metals can be more toxic than water-phase metals (Chen et al., 2016, 2017; Yan et al., 2012; Zheng et al., 2015). ZnO NPs produce oxidative stress and inhibit antioxidant mechanisms, particularly in hepatic and kidney cells (Xiao et al., 2016; Yao et al., 2019), and induce inflammation in the hepatic and kidney (Almansour et al., 2019; Tang et al., 2016). In the aquatic environment, ZnO NPs cause significant oxidative stress and organ damage in carp (*Cyprinus carpio*) (Hao et al., 2013), zebrafish (*Danio rerio*) (Xiong et al., 2011), and nile tilapia (Kaya et al., 2015), thus jeopardizing the health of aquatic organisms. Moreover, ZnO NPs induce hepatic oxidative stress, leading to alterations in antioxidant enzyme activities (Mahjoubian et al., 2023) and the levels of apoptosis-related genes in the liver, resulting in apoptosis and structural changes in the hepatic tissue (Daei et al., 2023). Dietary addition of ZnO NPs also disrupts hepatic zinc metabolism, increases lipid accumulation, and downregulates lipolysis (Chen et al., 2022; Mawed et al., 2022).

The rare minnow (*Gobiocypris rarus*) is a small freshwater fish endemic to China, known for its long reproductive cycle, rapid sexual maturity, continuous spawning, and wide temperature tolerance (Wang and Cao, 2017). The rare minnow, known for its high sensitivity to pollutants, is extensively utilized in pollutant risk assessments in China. It is a native model fish recommended by China's national standard (GB/T29763–2013) for monitoring environmental pollutants in water quality. Previous studies have shown that excess zinc causes developmental toxicity in rare minnow embryos (Zhu et al., 2014). However, the hepatotoxic effects of ZnO NPs on the rare minnow have not been previously reported.

This study examined the impact of dietary ZnO NPs on hepatic lipid metabolism, oxidative stress and apoptosis in rare minnow through histopathology, enzyme activities, and gene and protein levels in the liver. This research aims to enhance the understanding of the risks associated with adding ZnO NPs to feed and elucidate the mechanisms of hepatotoxicity induced by dietary ZnO NPs, focusing on reactive oxygen species (ROS)-mediated activation of oxidative stress, apoptosis and inhibition of lipid peroxidation.

2. Materials and methods

2.1. Experimental animals and culture

In this research, 300 healthy mature rare minnows (1.2 ± 0.2 g per fish, nine months old) were obtained from the National Aquatic Biological Resource Center (NABRC). These minnows were acclimated for one week in eight-liter seamless glass tanks and no instances of mortality were observed. Throughout both the acclimatization and experimental periods, a consistent 12-hour light-dark photoperiod (08:00 – 20:00) was maintained. Water quality was carefully monitored, with each six-liter tank being refreshed twice daily to ensure optimal conditions, including temperature (25 – 27 ℃), pH (7.0 – 8.5), and dissolved oxygen levels (7 – 9 mg/L). The minnows were provided with a basal diet twice daily until satiety, with the ingredient composition detailed in Table S1 of the Supporting Information. All experiments received approval from the Ethics Committee of Wuhan Polytechnic University (approval number WPUF20221008, approval date 8 October 2022).

2.2. Experimental design

After one week of acclimatization, 300 healthy and mature rare minnows were randomly selected for use in this experiment. Based on the results of previous studies on sub-chronic toxicity of 7 d larvae (Unpublish) and Shukry et al. (2022), 20 mg/kg and 60 mg/kg ZnO NPs were used as the dose of this experiment. Generally, this experiment was randomly assigned to three groups: the control group (basal diet + 0 mg/kg ZnO NPs), the N-20 group (basal diet + 20 mg/kg ZnO NPs), and the N-60 group (basal diet + 60 mg/kg ZnO NPs). Each group was housed in 10 seamless glass tanks (n = 10 per tank). ZnO NPs at 0, 20 and 60 mg/kg were added to the feed ingredients, mixed thoroughly and then made into 1 mm pellets using a laboratory granulator. The pellets were air-dried at 25 ℃ for 24 hours and then crushed, passed through a 24-mesh sieve and stored at 4 ℃. ZnO NPs (99.9 % metals basis) were obtained from Shanghai MACKLIN Biochemical Technology Co. (Shanghai, China). The experimental period lasted for 60 days. Following feeding durations of 15, 30, 45, and 60 days, 25 fish from each cohort were euthanized using a solution of 200 mg/L MS-222 (Shanghai Adamas Reagent Co., Ltd., Shanghai, China) for body weight measurement and rapid dissection for hepatic tissues. Five hepatic tissues from each group were weighed to calculate the hepato-somatic index (HSI). These hepatic tissues were then used for subsequent testing. Feeding was suspended 12 hours before sampling. During the acclimatization and experimental periods, water quality parameters were consistently maintained at a temperature of 25.8 ± 0.95 ℃, a pH level of 8.32 ± 0.21, and a dissolved oxygen concentration of 8.29 ± 0.52 mg/L. The nutritional composition of the feeds for each experimental group is presented in Table 1. The crude protein, ether extract, ash and moisture in the experimental diet were analyzed in accordance with standards GB/T 6435–2014, GB/T 6432–2018, GB/T 6433–2006, and GB/T 6438–2007, respectively.

2.3. Analyses of Zn content in hepatic tissues of rare minnow and experimental diets

The zinc concentration in the liver of the rare minnow was determined utilizing inductively coupled plasma mass spectrometry (ICP-MS) (PerkinElmer NexION 300X; Pekin Elmer, Waltham, MA, USA). One liver sample of rare minnow and 0.05 g feed ration from each group were digested separately in a microwave digestion system with 200 μL of HNO_3 and incubated at 65 ℃ for 24 hours. Liver and feed samples were analyzed in three replicates (n = 3). Following the digestion process, the addition of 9.8 mL of deionized water achieved a final volume of 10 mL, resulting in a 2 % concentration of HNO_3. Subsequently, the samples underwent analysis utilizing HPLC-ICP-MS. The detection limit was 0.01 μg/g dry weight, with recoveries ranging from 96 % to 98 %. Zinc concentration in the liver was expressed as μg/g dry weight. The results were reported as the average values accompanied by their respective standard deviations (SD).

2.4. Assessment of hepatic injury

Paraformaldehyde-fixed hepatic samples were paraffin-embedded to visualize hepatic damage and stained with hematoxylin and eosin (H&E). Each group consisted of three liver tissue samples that were dissected and then fixed in paraformaldehyde at 4 ℃ for 24 hours. After fixation, the liver samples were graded, dehydrated in an ethanol series, and embedded in paraffin following standard histological procedures. Thick Section (5 μm) were cut from the paraffin blocks using a rotary microtome and stained with H&E. The sections were examined utilizing

Table 1
Nutritional levels in the diets of experimental groups fed with rare minnow basal diet + 0 mg/kg ZnO NPs (The control group), basal diet + 20 mg/kg ZnO NPs (The N-20 group), and basal diet + 60 mg/kg ZnO NPs (The N-60 group) (%, dry weight basis).

Items	Measured Content (%, dry weight basis)		
	The control group	The N-20 group	The N-60 group
Crude protein	39.96 ± 0.46	39.24 ± 0.47	39.30 ± 0.49
Ether extract	6.08 ± 0.17	7.00 ± 0.72	7.21 ± 0.32
Ash	6.348 ± 0.73	6.94 ± 0.09	6.66 ± 0.47
Moisture	8.85 ± 0.11	8.43 ± 0.38	8.39 ± 0.11

Data are measured as mean ± standard deviation.

an Olympus CX33 light microscope (Olympus Corporation, Tokyo, Japan) equipped with a camera. The staining of the sections was performed by Wuhan Service Bio Technology Co., Ltd (Wuhan, China).

To compare the degree of hepatic tissue injury caused by ZnO NPs, the liver injury status index (I_h) was estimated according to the weighted index method proposed by Bernet et al. (1999) for fish with modifications. All experiments were analyzed in three replicates. This method accounts for the biological significance (weights) of each observed alteration and its degree of spread (score). Weight values ranged between 1 and 3 (most severe), and scores ranged from 0 (no features/alterations observed) to 6 (diffuse). The liver injury status index was calculated using the following formula:

$$I_h = \sum_1^j w_j \quad a_{jh}$$

where I_h is the liver injury status index for the individual h; w_j is the weight of the *j*th liver injury status alteration and a_{jh} the score attributed to the *h*th individual for the *j*th alteration.

2.5. Hepatic lipid profile

One liver sample from each group was homogenized with 0.45 mL of hypothermic PBS at a milling frequency of 60.00 Hz, a milling run time of 30 seconds, a milling interruption of 10 seconds, and two milling runs at a milling run temperature of 4℃ (n = 3 replicates per group, 1 liver sample per replicate). The homogenates were centrifuged at 3500 rpm at 4 ℃ for 15 minutes to obtain a 10 % hepatic tissue supernatant. Protein levels were examined utilizing the BCA protein assay kit (Nanjing Jiancheng, Nanjing, China). The hepatic lipid profile was assessed utilizing 10 % liver tissue homogenate. Total cholesterol (T-CHO), triglyceride (TG), lipoprotein lipase (LPL), and hepatic lipase (HL) levels were detected using kits from Nanjing Jiancheng Bioengineering Institute (Nanjing, China). Enzyme-linked immunosorbent assay (ELISA) kits for fish acetyl CoA carboxylase (ACC) and fatty acid synthase (FAS) were obtained from Jiangsu Meimian Industrial Co., Ltd (Jiangsu, China). The ACC and FAS levels were quantified following the manufacturer's guidelines.

2.6. Detection of reactive oxygen species (ROS) in hepatic of rare minnow

ROS was analyzed through fluorescence intensity quantification to observe liver oxidative stress levels. One liver sample from each group was rinsed in pre-cooled PBS, and 2 mL of 0.25 % trypsin was added to digest for 5 minutes at 37 ℃ (n = 3 replicates per group, 1 liver sample per replicate). The cells were collected by filtering through an 80-mesh cell sieve to remove tissue clumps. The cells were labeled with a 2,7-dichlorpfuorescin diacetate (DCFH-DA) probe, incubated for 1 hour at 37 ℃, and then centrifuged at 941 rpm for 5 minutes to collect the cell precipitate. The cells were resuspended in PBS and analyzed for ROS levels at an excitation wavelength of 488 nm and an emission wavelength of 525 nm. ROS levels were detected using a kit produced by Nanjing Jiancheng Bioengineering Institute (Nanjing, China).

2.7. Determination of antioxidant capacity

Two randomly selected liver samples from each group were homogenized in a mixture of 0.9 mL of low-temperature PBS, with a milling frequency of 60.00 Hz, a milling run time of 30 seconds, a milling interruption of 10 seconds, two milling runs, and a milling run temperature of 4 ℃ (n = 3 replicates per group, 2 liver samples per replicate). The homogenates were centrifuged at 3500 rpm at 4 ℃ for 15 minutes to obtain a 10 % hepatic tissue supernatant. Protein content was determined using the BCA protein assay kit (Nanjing Jiancheng, Nanjing, China). Hepatic antioxidant status-related indicators, such as total antioxidant capacity (T-AOC), catalase (CAT), total superoxide dismutase (T-SOD), glutathione peroxidase (GSH-PX) and malondialdehyde (MDA), were determined according to Zhang et al. (2024) and Liu et al. (2023) and were measured and calculated according to the kit procedures from Nanjing Jiancheng Bioengineering Institute (Nanjing, China).

The activity of T-AOC was determined by the colorimetry method. The T-AOC unit in tissue was defined as per milligram of tissue protein per minute increased the absorbance (OD) value of the reaction system at 37 ℃ for 0.01 as 1 unit of T-AOC activity (U/mgprot). The activity of CAT was determined by the ammonium molybdate method. The CAT unit in tissue was defined as per milligram of tissue protein broken down 1 μmol of H_2O_2 per second as 1 unit of enzyme activity (U/mgprot). The activity of T-SOD was determined by the water-soluble tetrazolium salt-1 (WST-1) method. The T-SOD unit in tissue was defined as when the T-SOD inhibition rate per milligram of tissue protein reached 50 % in a reaction solution volume of 1 mL, the corresponding T-SOD amount was 1 unit of T-SOD activity (U/mgprot). The activity of GSH-PX was determined by the colorimetry method. The GSH-PX unit in tissue was defined as per milligram of tissue protein per minute reduced the concentration of GSH in the reaction system by 1 μmol/L at 37 ℃ as 1 unit of enzyme activity (U/mgprot). The content of MDA (nmol / mgprot) was determined by the thiobarbituric acid (TBA) method.

2.8. Quantitative real-time PCR (qRT-PCR) analysis

Total RNA was isolated from the liver samples of rare minnows (n = 3 replicates per group, 1 liver sample per replicate). Following the method of Rio et al. (2010), homogenization was performed in 5 mL of Trizol reagent (Invitrogen, Carlsbad, CA, USA), followed by RNA extraction. The quality of the extracted RNA was assessed by measuring optical density at 260 and 280 nm utilizing spectrophotometry (Thermo Fisher Scientific, Waltham, MA, USA). Subsequently, 1 μg of total RNA was reverse-transcribed into cDNA utilizing Moloney murine leukemia virus (M-MLV) reverse transcriptase (Yudhi et al., 2024) (Sangon Biotech, Shanghai, China) and oligo d(T) primers, resulting in a final reaction volume of 20 μL. The synthesized cDNAs were stored at - 20 ℃ for RT-PCR analysis.

RT-PCR analysis was carried out utilizing a SYBR Green PCR master mix (Bimake, Houston, TX, USA) on a fluorescence quantitative PCR instrument from Bio-Rad (California, USA). Each reaction mixture consisted of 10 μL SYBR Green PCR master mix, 7 μL nuclease-free water, 2 μL cDNA (100 ng), and 0.5 μL of each primer. The PCR protocol included an initial denaturation at 95 ℃ for 5 minutes, followed by 40 cycles of denaturation at 95 ℃ for 10 seconds, annealing at 60 ℃ for 10 seconds, and extension at 72 ℃ for 30 seconds. A subsequent dissociation curve analysis was performed to verify single-product amplification at the completion of each PCR run. All reactions were run in triplicate. The reference gene β-actin was employed as an internal control to normalize the expression levels of the target genes, which were evaluated using the comparative threshold cycle method ($2^{-\triangle\triangle Ct}$ method). Detailed primer sequences for the RT-PCR analysis can be found in Table S2 of the Supporting Information.

2.9. Western blot (WB) analysis

Liver samples from each group (n = 3 replicates per group, 1 liver sample per replicate) were utilized for protein extraction. Hepatic protein was extracted utilizing ice-cold RIPA lysis buffer containing 1 % triton X-100, 1 % sodium deoxycholate, 0.1 % SDS, and protease inhibitors (CWBIO, Beijing, China). Protein concentration was examined through the BCA method. Proteins (30 μg) were separated by 10 % SDS-PAGE and transferred to polyvinylidene fluoride membranes (Millipore, Billerica, USA). Membranes were probed with rabbit anti-Nrf2, anti-P53, and anti-Srebp-1 (all 1:1000, Wanlei, China), and mouse anti-β-actin (1:2000, Guanxing Yun Sci&Tech Co., Beijing, China). Anti-β-actin served as the loading control. The blots were probed with horseradish peroxidase-conjugated secondary antibodies (anti-rabbit 1:1500, anti-

mouse 1:3000, Beyotime, Jiangsu, China). Immunoreactive bands were visualized using ECL reagents (Advansta, California, USA) and analyzed with a ChemiDoc XRS+ imaging system (Bio-Rad, California, USA) and ImageJ 1.48 software.

2.10. Statistical analyses

Statistical analyses were conducted utilizing SPSS version 19.0 (IBM, Armonk, NY, USA). The normality and homogeneity of variance were evaluated using the Kolmogorov-Smirnov and Levene tests, respectively. Upon the fulfillment of the normality and homogeneity assumptions, the data were analyzed using one-way analysis of variance (ANOVA) followed by Tukey's HSD post hoc test for multiple comparisons. Data significance was determined at $P < 0.05$. The results were reported as mean ± SD. Graphs were generated utilizing GraphPad Prism version 7.0 (GraphPad Software Inc., La Jolla, USA).

3. Results

3.1. Effects of ZnO NPs on body weight and HSI

Dietary supplementation with ZnO NPs reduced body weight in rare minnow (Fig. 1a). At 60 d, the weight of fish in the control group was 1.2 ± 0.04 g, while the weight of fish in N-20 and N-60 groups was significantly reduced to 0.93 ± 0.01 g and 0.88 ± 0.07 g ($P < 0.05$). Similarly, dietary supplementation of ZnO NPs reduced the HSI of rare minnow (Fig. 1b). At 60 d, the HSI of fish in the control group was 1.61 % ± 0.12 % whereas the HSI of fish in the N-20 and N-60 groups was significantly lower at 1.06 % ± 0.16 % and 1.11 % ± 0.12 % ($P < 0.05$).

3.2. Effect of ZnO NPs on Zn content in the hepatic tissues and experimental group feed

Dietary supplementation with ZnO NPs altered Zn contents in the hepatic tissues of rare minnow. The Zn contents in control fish ranged from 38.54 μg/g to 39.21 μg/g. In the ZnO NPs-fed groups, Zn content significantly increased compared to control levels ($P < 0.05$, Table 2).

3.3. Effects of ZnO NPs on hepatic histological indices

Control fish exhibited normal hepatocyte structure, characterized by large nuclei, stained dark blue-purple, centrally located in hepatocytes, fewer and visible hepatic blood sinusoids, and clear red blood cells in microvessels (Figs. 2a, 2d, 2g and 2j). However, N-20 and N-60 groups showed pathological features, including severe vacuolization of hepatocytes, loss of hepatocyte shape, swelling of hepatocytes, and displacement of nuclei in some cells (Figs. 2b-c, 2e-f, 2h-i and 2k-l). The liver injury status index exhibited a significant increase in the treatment groups ($P < 0.05$, Table 3).

Table 2
Zn content in the hepatic tissues of rare minnow after dietary supplement with basal diet + 0 mg/kg ZnO NP (Control group), basal diet + 20 mg/kg ZnO NPs (N-20 group) and basal diet + 60 mg/kg ZnO NPs (N-60 group) for 15 d, 30 d, 45 d and 60 d, including actual measurements of Zn content in the diets of each treatment group.

samples		The concentration of ZnO NPs (μg/g dry weight)		
		Control group	N-20 group	N-60 group
hepatic tissues	15 d	38.54 ± 0.92^{a}	46.43 ± 3.08^{ab}	51.93 ± 4.27^{b}
	30 d	39.53 ± 1.67^{a}	49.10 ± 3.35^{b}	53.22 ± 2.11^{b}
	45 d	40.17 ± 0.83^{a}	50.90 ± 2.25^{b}	52.57 ± 2.08^{b}
	60 d	39.21 ± 1.61^{a}	52.11 ± 3.07^{b}	55.43 ± 2.24^{b}
experimental group feed		66.62 ± 1.46^{a}	78.39 ± 1.78^{b}	84.89 ± 1.48^{c}

Different letters in the same column indicate significant differences ($P < 0.05$). Values are measured as mean ± standard deviation.

3.4. Effects of ZnO NPs on hepatic lipid profile in rare minnow

Dietary supplement with ZnO NPs increased T-CHO and TG levels in hepatic tissues overall, with significantly differences in T-CHO levels at feeding for 15 and 45 days ($P < 0.05$, Fig. 3a). Except for the N-60 group at 15 days and the N-20 group at 45 days, TG contents generally elevated in ZnO NPs-treated groups than in the control levels ($P > 0.05$, Fig. 3b). For LPL, dietary ZnO NPs at 20 mg/kg and 60 mg/kg significantly inhibited its activity at 15 and 30 days ($P < 0.05$), but significantly improved it at 45 and 60 days ($P < 0.05$, Fig. 3c). For HL, dietary ZnO NPs significantly altered its activity in hepatic tissues ($P < 0.05$, Fig. 3d). However, the opposite trend was observed in the 60 mg/kg ZnO NPs-treated group, showing a decrease followed by a significant increase ($P > 0.05$, Fig. 3e). After ZnO NPs feeding, FAS content in liver tissues initially decreased significantly and then slowly increased ($P < 0.05$, Fig. 3f). In ACC research, the activity of hepatic tissues showed an initial increase after dietary supplementation with 20 mg/kg of ZnO NPs within the first 30 days, followed by a subsequent decline There was no statistically significant distinction detected between the treatment group and the control group ($P > 0.05$, Fig. 3e). In contrast, a different pattern was observed in the group treated with 60 mg/kg of ZnO NPs. Specifically, the ACC content significantly rose after 60 days of treatment ($P < 0.05$, Fig. 3e). FAS content in hepatic tissues initially reduced and then increased, with higher levels found in the hepatic tissues of rare minnow fed ZnO NPs for 60 days ($P < 0.05$, Fig. 3f).

3.5. Effects of ZnO NPs on antioxidant enzyme in rare minnow hepatic tissues

Dietary supplementation with 20 mg/kg ZnO NPs for 15, 45 and 60 days significantly increased ROS production in the hepatic tissues ($P < 0.05$, Fig. 4a). However, a notable decrease in ROS levels was observed in the group supplemented for 60 days ($P < 0.05$, Fig. 4a). Compared to control levels, T-SOD and CAT activities generally increased in the ZnO

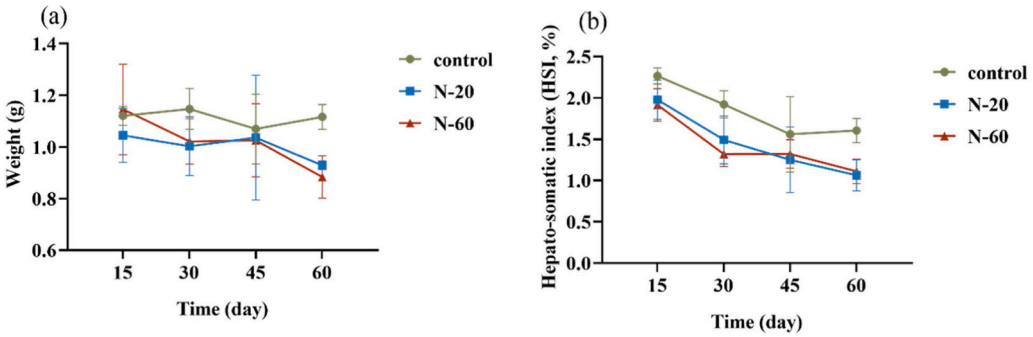

Fig. 1. Body weight and hepato-somatic index (HSI) of rare minnow after dietary supplement of 0 mg/kg, 20 mg/kg and 60 mg/kg ZnO NPs for 15 d, 30 d, 45 d and 60 d (n = 3). (a) Weights of rare minnow. (b) HSI of rare minnow.

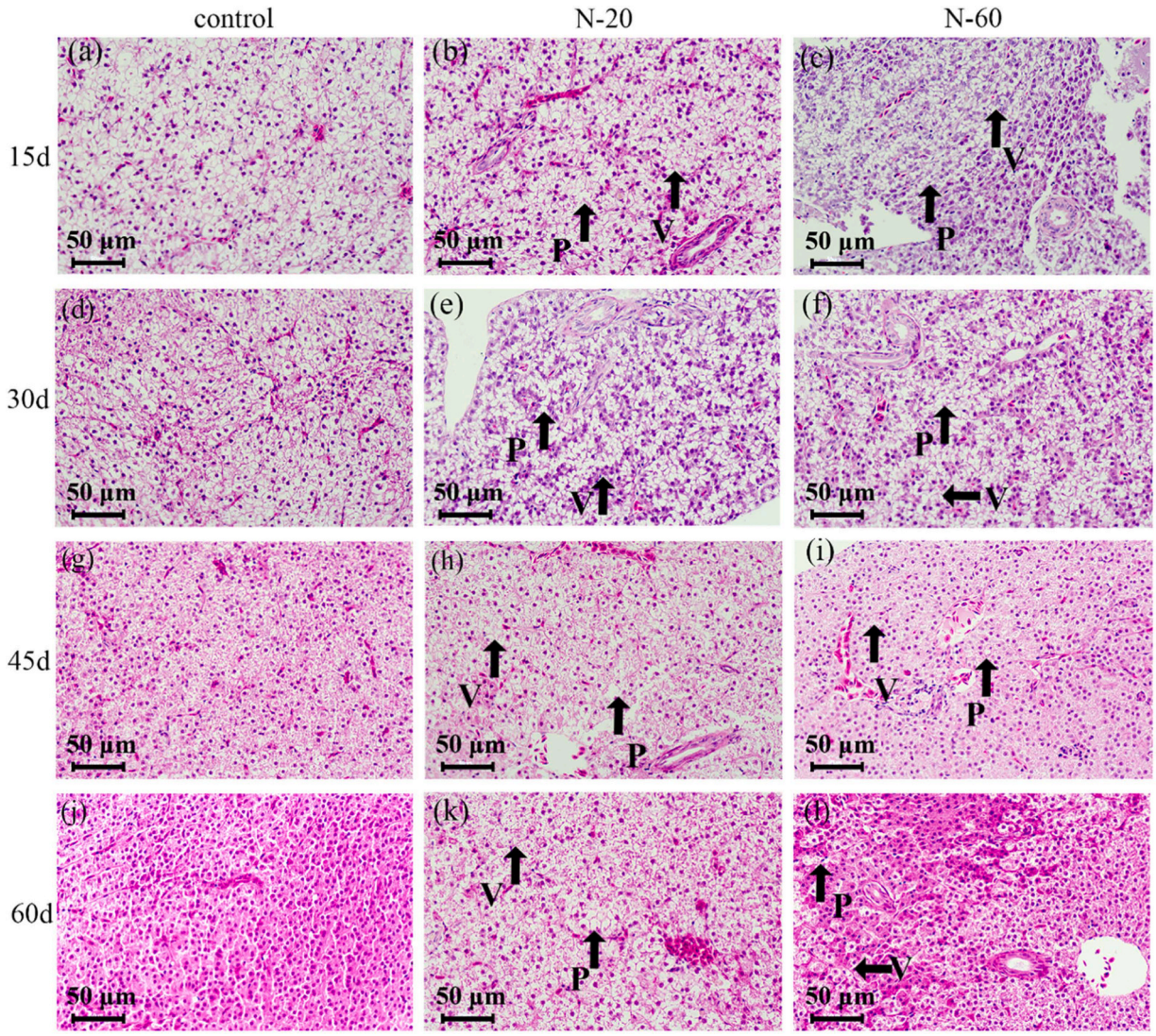

Fig. 2. Hepatic tissues of rare minnow after dietary supplement of 0 mg/kg, 20 mg/kg and 60 mg/kg ZnO NPs (n = 3). (a, d, g, j) Normal hepatic tissues (fed with the control diet for 15 d,30 d,45 d and 60 d, respectively). (b, e, h, k) Hepatic tissues of 20 mg/kg ZnO NPs-fed group (fed with the N-20 diet for 15 d,30 d, 45 d and 60 d, respectively). (c, f, i, l) Hepatic tissues of 60 mg/kg ZnO NPs-fed group (fed with the N-20 diet for 15 d, 30 d, 45 d and 60 d, respectively). p = hepatocyte vacuolization; v = absence of nucleus.

Table 3
The liver injury status index of rare minnow supplemented with 0 mg/kg, 20 mg/kg and 60 mg/kg ZnO NPs in diets for 15 d, 30 d, 45 d and 60 d.

Feeding days (d)	I_h		
	Control group	N-20 group	N-60 group
15	4.67 ± 0.47^a	13.67 ± 0.47^b	17.67 ± 0.47^c
30	6.00 ± 0.82^a	15.00 ± 0.82^b	18.33 ± 0.94^c
45	5.33 ± 0.47^a	17.67 ± 0.47^b	18.00 ± 0.82^b
60	5.67 ± 0.47^a	17.33 ± 0.47^b	19.67 ± 0.47^c

Weight values ranged between 1 and 3 (most severe), and scores ranged from 0 (no features/alterations observed) to 6 (diffuse). $w = 1$: intercellular oedema and structural alterations, $w = 2$: nuclear alterations and atrophy, $w = 3$: necrosis and vacuolar degeneration. Different letters in the same column indicate significant differences ($P < 0.05$). Values are measured as mean ± standard deviation.

NPs-fed groups (Figs. 4b and 4c). Specifically, CAT activity significantly decreased in the N-60 group at 15 days ($P < 0.05$), and both T-SOD and CAT activities decreased in the N-20 group at 45 days. In the treated groups, T-AOC activities exhibited a general suppression when compared to those in the control group. GSH-PX activity in the N-20 group exhibited a pattern of activation-inhibition-activation-inhibition. The N-60 group showed activation-inhibition-activation, with significant inhibition at 14 days and significant activation at other times (Fig. 4e). Compared to the control group, MDA content was generally suppressed in the treated groups. However, MDA activity in the N-20 group significantly increased to 2.73 ± 0.07 nmol/mg at 30 days (Fig. 4f).

3.6. Effects of ZnO NPs on antioxidant response in rare minnow hepatic tissues

To further explore the potential mechanism of oxidative stress induced by dietary ZnO NPs, the levels of antioxidant defense-related genes was examined in the hepatic tissues of rare minnow. Nrf2 protein expression in rare minnow hepatic tissues was significantly altered in response to dietary ZnO NPs ($P < 0.05$, Figs. 5a and 5b). Specifically, supplementation of hepatic tissues with 20 mg/kg ZnO NPs initially led to an increase in Nrf2 protein expression, followed by a significant reduction ($P < 0.05$). In the N-60 group, Nrf2 protein levels increased at

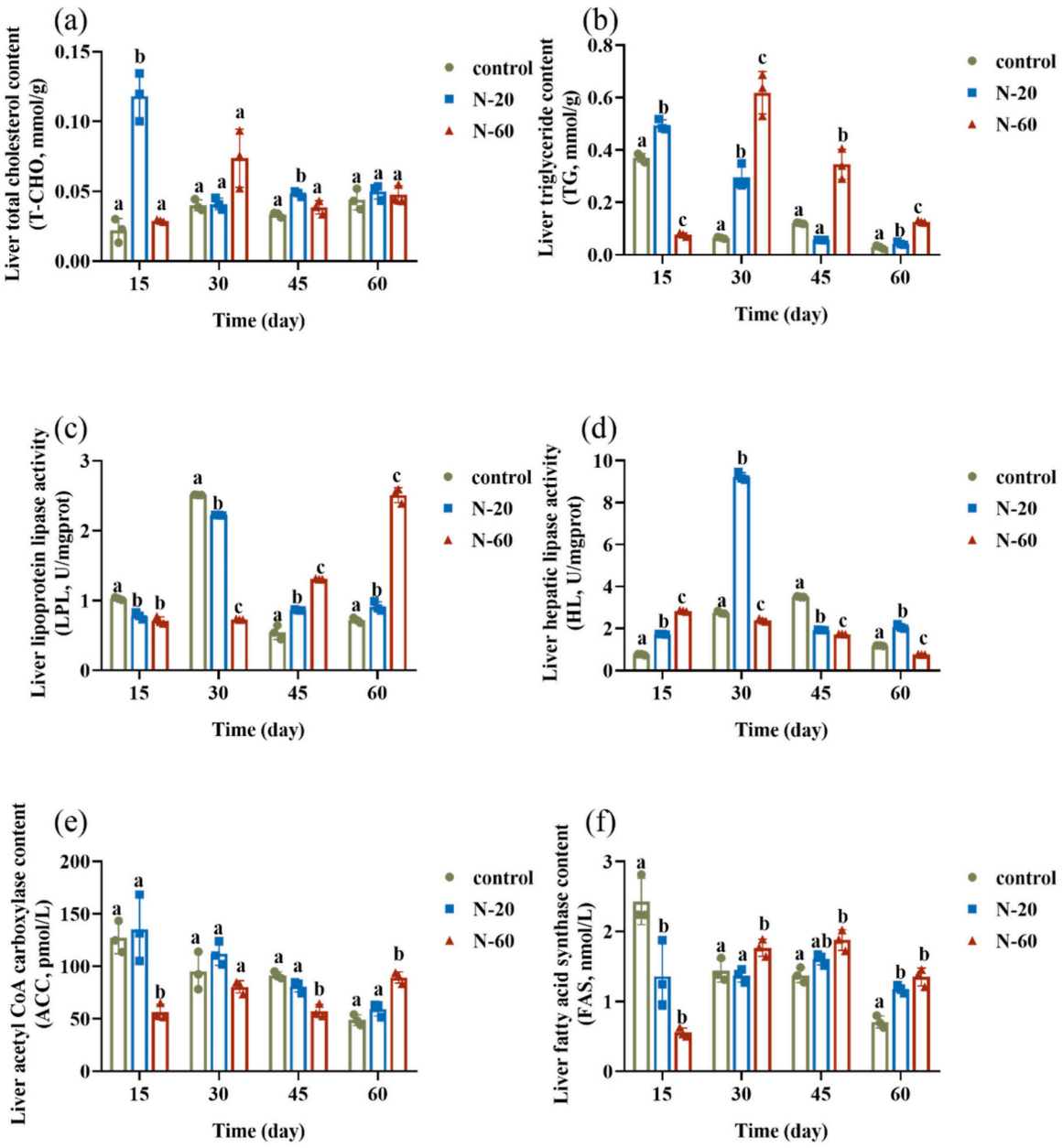

Fig. 3. Hepatic lipid metabolism of rare minnow after dietary supplement of 0 mg/kg (Control group), 20 mg/kg (N-20 group) and 60 mg/kg ZnO NPs (N-60 group) for 15 d, 30 d, 45 d and 60 d (n = 3). (a) Total cholesterol (T-CHO) content. (b) Triglyceride (TG) content. (c) Lipoprotein lipase (LPL) activity. (d) Hepatic lipase (HL) activity. (e) Acetyl CoA carboxylase (ACC) content. (f) Fatty acid synthase (FAS) content. Data are represented as mean ± standard deviation. Different letters indicate a statistically significant difference in the treated group compared to the control group ($P < 0.05$).

first, then decreased, and elevated significantly at 60 days ($P < 0.05$). The relative expression of *nrf2* in the hepatic tissues of rare minnow fed with 20 mg/kg ZnO NPs for 30 and 45 days was significantly lower than those fed the control diet ($P < 0.05$, Fig. 5e), but higher relative expression levels were found at 60 days ($P < 0.05$, Fig. 5e). Dietary supplement of ZnO NPs in rare minnow activated the antioxidant defense response in its hepatic tissues (Fig. 5c). The mRNA expression of *mn-sod*, *gclc*, *gpx1*, *cat*, and *nf-κb* were all significantly up-regulated in the N-60 group at 15 days. The mRNA expression of *mn-sod* in the ZnO NPs-treated group was upregulated. The mRNA levels of the Nrf2 signaling pathway positively correlated with the mRNA levels of *mn-sod*, *gclc*, *gpx1*, and *cat* in response to ZnO NPs (Fig. 5d).

3.7. Effects of ZnO NPs on apoptosis response in rare minnow hepatic tissues

To explore the potential mechanism of apoptosis induced by ZnO NPs, the levels of apoptosis-related genes in the liver tissues of rare minnow was examined. P53, a crucial regulator of apoptosis, significantly contributes to mediating the apoptosis pathway. Dietary supplementation with ZnO NPs significantly altered P53 protein expression in liver tissues (Figs. 6a and 6b). Specifically, P53 protein expression in the N-20 group was significantly reduced, except for a significant increase at 30 days of feeding ($P < 0.05$). In the N-60 group, P53 protein levels initially decreased significantly, then increased significantly, and finally decreased ($P < 0.05$). The relative levels of p53 in hepatic tissues of rare minnows fed 20 mg/kg ZnO NPs for 15, 30, and 45 days was significantly higher than control levels but significantly lower at 60 days. In

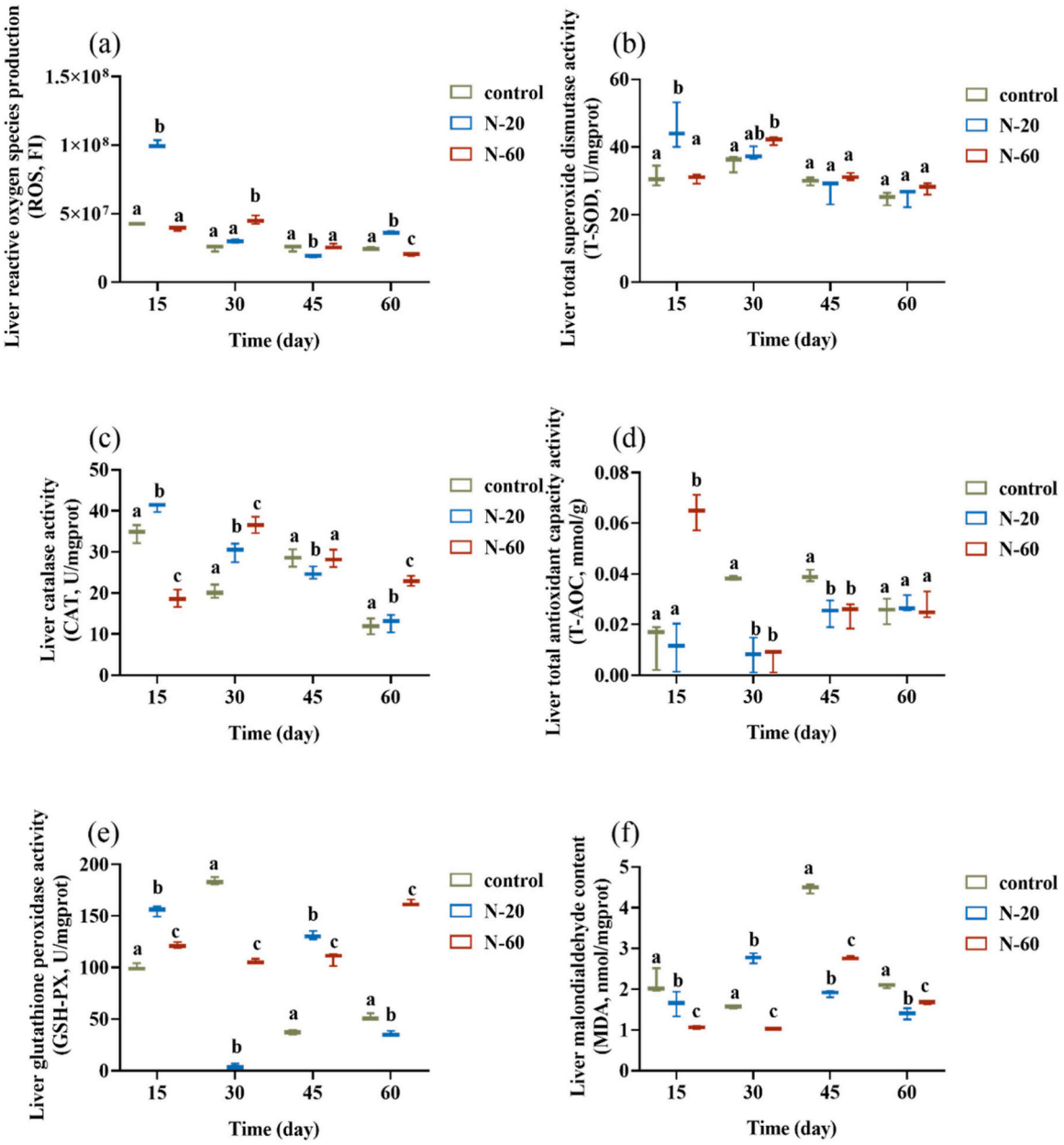

Fig. 4. Hepatic oxidative activities of rare minnow after dietary supplement of 0 mg/kg (Control group), 20 mg/kg (N-20 group) and 60 mg/kg ZnO NPs (N-60 group) for 15 d, 30 d, 45 d and 60 d (n = 3). (a) Reactive oxygen species (ROS) production. (b) Total superoxide dismutase (T-SOD) activity. (c) Catalase (CAT) activity. (d) Total antioxidant capacity (T-AOC) activity. (e) Glutathione peroxidase (GSH-PX) activity. (f) Malondialdehyde (MDA) content. Data are represented as mean ± standard deviation. Different letters indicate a statistically significant difference in the treated group compared to the control group ($P < 0.05$).

the N-60 group, p53 gene expression was significantly downregulated except at 30 days ($P < 0.05$, Fig. 6e). ZnO NPs ingestion activated the apoptotic response in liver tissues of rare minnow (Fig. 6c). The mRNA expression of *casp3*, *casp8*, *casp9*, *bcl2*, and *bax* was significantly up-regulated in the N-20 group at 30 days. The mRNA expression of *bax* was up-regulated in the ZnO NPs-treated group. The mRNA levels of *p53* signaling pathway were significantly and positively correlated with the mRNA levels of *casp3*, *casp8*, *casp9* and *bcl2* ($P < 0.05$, Fig. 6d).

3.8. *Effects of ZnO NPs on lipid metabolism response in rare minnow hepatic tissues*

To explore the potential mechanism of ZnO NPs-induced lipid metabolism changes, the expression of lipid metabolism-related genes in the liver tissues of rare minnow was examined. Srebp1 protein expression in liver tissues was significantly altered by dietary ZnO NPs (Figs. 7a and 7b). Specifically, Srebp1 protein in the N-20 group significantly increased at 15 and 45 days of feeding ($P < 0.05$) and slightly decreased at 30 and 60 days of feeding ($P < 0.05$). In the N-60 group, Srebp1 protein initially elevated and then significantly decreased ($P < 0.05$). The relative expression of *srebp1* in the N-20 group was initially upregulated and then downregulated after 30 days. In the N-60 group, *srebp1* mRNA levels were significantly upregulated initially and then significantly downregulated after 45 days ($P < 0.05$, Fig. 7e). ZnO NPs ingestion activated and then inhibited the lipid metabolic response in the liver tissue (Fig. 7c). The mRNA expression of *tpi1*, *pgk1*, *dgat1a*, *dgat1b*, *acaca*, *acacb*, *fasn*, *gpat1* and *gpat3* was significantly down-regulated in the N-20 group at 30 days. In response to ZnO NPs, the mRNA levels of the *srebp1* signaling pathway demonstrated a notable positive correlation with the mRNA levels of *tpi1*, *dgat1a*, *fasn*, and *gpat3*

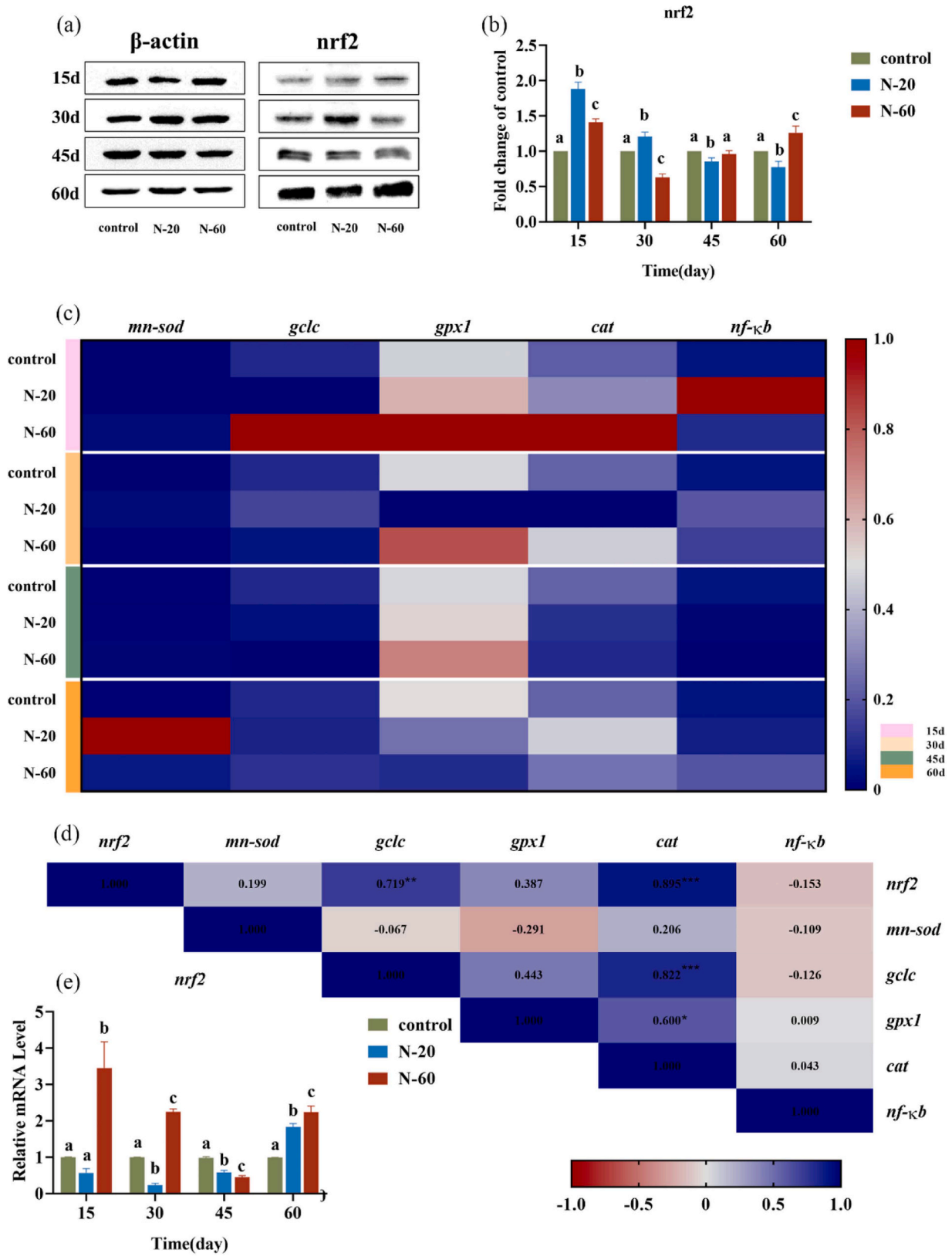

Fig. 5. Hepatic antioxidant response of rare minnow after dietary supplement of 0 mg/kg (Control group), 20 mg/kg (N-20 group) and 60 mg/kg ZnO NPs (N-60 group) for 15 d, 30 d, 45 d and 60 d (n = 3). (a) Relative protein expressions of Nrf2. (b) Relative expression of Nrf2 protein normalized to β-actin. (c) Heatmap of relative mRNA levels of *nrf2* and its downstream genes. mRNA levels of *nrf2* relative genes are shown using the indicated pseudo color scale from 1.0 (red) to 0 (blue) relative to values for hepatic in the control group. The color scale represents the relative mRNA levels. (d) Correlation analysis of the mRNA levels of *nrf2* and its downstream genes (* $P < 0.05$, ** $P < 0.01$, *** $P < 0.001$). (e) Relative mRNA level of *nrf2*. Data are represented as mean ± standard deviation. Different letters indicate a statistically significant difference in the treated group compared to the control group ($P < 0.05$).

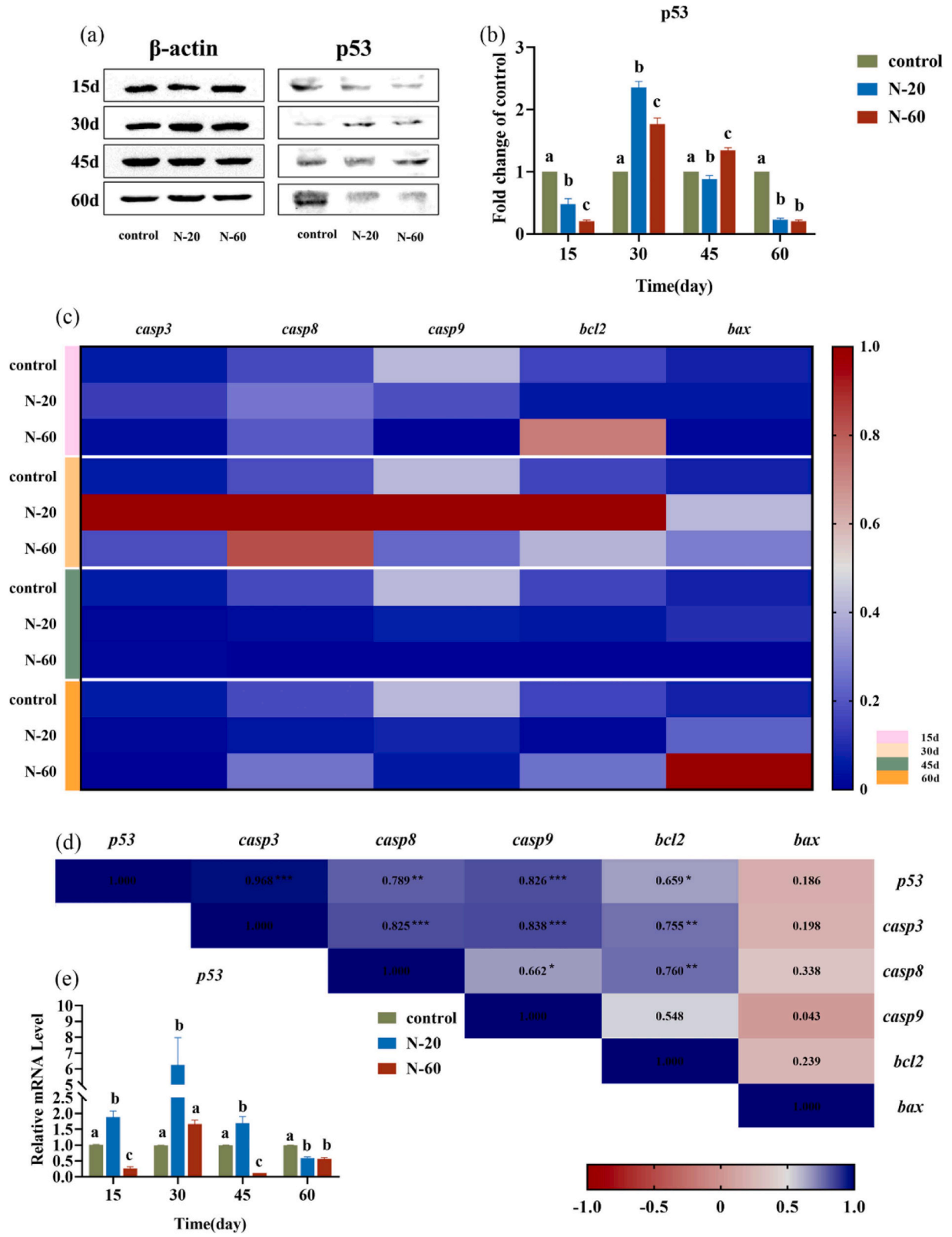

Fig. 6. Hepatic apoptosis response of rare minnow after dietary supplement of 0 mg/kg (Control group), 20 mg/kg (N-20 group) and 60 mg/kg ZnO NPs (N-60 group) for 15 d, 30 d, 45 d and 60 d (n = 3). (a) Relative protein expressions of P53. (b) Relative expression of P53 protein normalized with β-actin. (c) Heatmap of relative mRNA levels of *p53* and its downstream genes. mRNA levels of *p53* relative genes are shown using the indicated pseudo color scale from 1.0 (red) to 0 (blue) relative to values for hepatic in the control group. The color scale represents the relative mRNA levels. (d) Correlation analysis of the mRNA levels of *p53* and its downstream genes (* $P < 0.05$, ** $P < 0.01$, *** $P < 0.001$). (e) Relative mRNA level of *p53*. Data are represented as mean ± standard deviation. Different letters indicate a statistically significant difference in the treated group compared to the control group ($P < 0.05$).

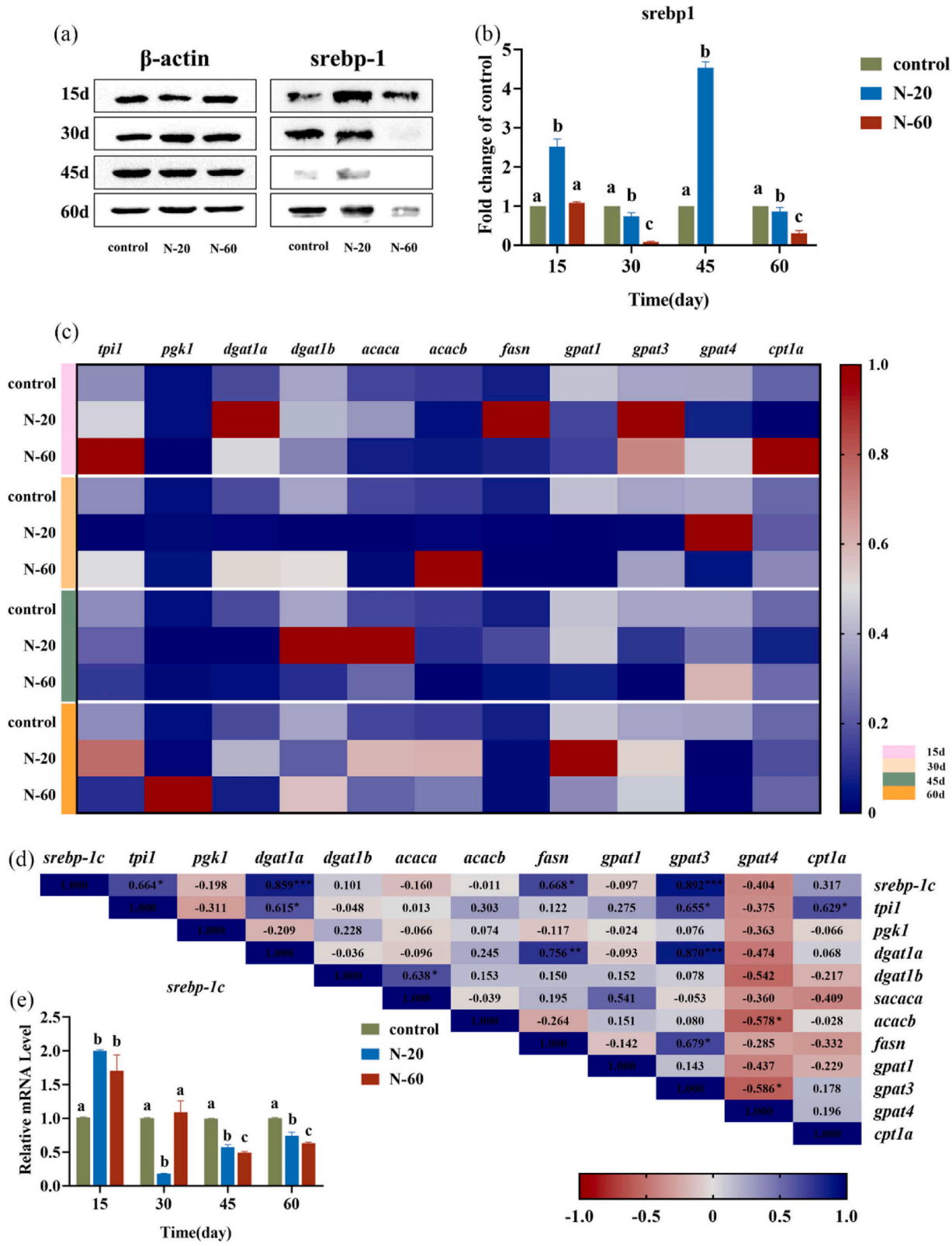

Fig. 7. Hepatic lipid metabolic response of rare minnow after dietary supplement of 0 mg/kg (Control group), 20 mg/kg (N-20 group) and 60 mg/kg ZnO NPs (N-60 group) for 15 d, 30 d, 45 d and 60 d (n = 3). (a) Relative protein expressions of Srebp1. (b) Relative expression of Srebp1 protein normalized with β-actin. (c) Heatmap of relative mRNA levels of *srebp1c* and its downstream genes. mRNA levels of *srebp1c* relative genes are shown using the indicated pseudo color scale from 1.0 (red) to 0 (blue) relative to values for hepatic in the control group. The color scale represents the relative mRNA levels. (d) Correlation analysis of the mRNA levels of *srebp1c* and its downstream genes (* $P < 0.05$, ** $P < 0.01$, *** $P < 0.001$). (e) Relative mRNA level of *srebp1c*. Data are represented as mean ± standard deviation. Different letters indicate a statistically significant difference in the treated group compared to the control group ($P < 0.05$).

($P < 0.05$, Fig. 7d).

4. Discussion

In this study, rare minnows that were exposed to 20 mg/kg and 60 mg/kg ZnO NPs for 60 days exhibited a reduction in body weight. The HSI values were measured at 1.06 ± 0.16 % and 1.11 ± 0.12 %, respectively, which were significantly lower compared to the control group. These findings are consistent with those reported by Pourmoradkhani et al. (2023) and Rajkumar et al. (2022). ZnO NPs may compete with other nutrients in the gut and reduce their absorption (Moreno-Olivas et al., 2019), thus affecting fish growth and body weight. The toxic effects of ZnO NPs may lead to a decrease in the activity level of fish (De Souza et al., 2018), affecting their predatory and feeding behavior and thus body weight. Generally, ZnO NPs are absorbed primarily as zinc and partially as particles, increasing zinc content in hepatic tissues (Fujihara and Nishimoto, 2023). Thus, the decreased HSI and weight loss in rare minnows may be due to the elevated zinc content caused by dietary ZnO NPs, which can increase lipid accumulation and down-regulate lipolysis, as evidenced by the deepening of hepatic color and weight loss in rare minnow.

In rare minnow, dietary supplementation with ZnO NPs caused hepatic injury, including extensive cytoplasmic vacuolization, focal necrosis, and irregular or absent nuclei in hepatic tissues. Similar phenomena were observed in gilthead seabream (*Sparus aurata*) (Izquierdo et al., 2017) and nile tilapia (Mohammady et al., 2021). Similar to the findings of Zhuo et al. (2024) and Farag et al. (2023), this study also found significantly elevated ROS production in liver tissue. ZnO NPs in organisms can release zinc ions, elevating ROS production (Bordin et al., 2024; Chong et al., 2021). ZnO NPs stand as among the most significant metal oxide nanoparticles in trigger the formation of ROS and induce apoptosis (Mishra et al., 2017). ROS are oxidizing free radicals produced by mitochondria during metabolic processes, and their excessive presence in tissues induces oxidative stress, promoting apoptosis and exacerbating liver injury (Li et al., 2023). Excessive production of ROS can lead to liver lesions such as hepatitis and fatty liver, further exacerbating liver damage and malfunctions. Thus, the hepatic injury in rare minnow caused by dietary ZnO NPs supplementation might be attributed to extensive ROS production.

Oxidative stress, resulting from the imbalance between ROS generation and detoxification, is crucial in determining cell fate. In response to excess ROS, apoptotic signaling pathways are activated to promote normal cell death (Sajadimajd and Khazaei, 2018). The heightened reactivity and enhanced cellular uptake of ZnO NPs can result in toxicity at high concentrations (Ma et al., 2013). ZnO NPs induce oxidative stress and elevate ROS formation, leading to the loss of mitochondrial membrane potential, lysosomal activity, nuclear cohesion, and ultimately apoptosis (Reshma and Mohanan, 2017). Similar to the findings of Chen et al. (2022), ZnO NPs up-regulated the expression of *nrf2* genes and proteins, and the expression of genes related to antioxidant (*mn-sod*, *cat* and *nf-κb*) in rare minnow liver further indicated that dietary supplements with ZnO NPs could cause oxidative stress, resulting in hepatic injury. Under oxidative stress, cells activate antioxidant responses to neutralize ROS (Poljsak et al., 2013). Nrf2 is a key transcription factor that responds to oxidative stress (Ma, 2013) by regulating the expression of antioxidant enzyme genes, such as *mn-sod* and *cat*. The up-regulation of *nrf2* suggests that the cell is attempting to resist oxidative stress, but excessive oxidative stress may be more than the antioxidant system is able to handle.

Excessive ROS may disrupt the mitochondrial membrane and affect mitochondrial function, including ATP production and cellular energy supply (Nolfi-Donegan et al., 2020). Impaired mitochondrial function may also release pro-apoptotic factors, further exacerbating apoptosis. P53 is a key player in mitochondria-mediated apoptotic cell death, promoting the levels of various pro-apoptotic genes and inducing cell growth arrest or apoptosis (Nayak et al., 2009). Through the upregulation of pro-apoptotic proteins Bax and Bak, P53 protein inhibits Bcl-2 activity to facilitate apoptosis. P53 activates the apoptotic pathway by affecting the integrity of the mitochondrial membrane and releasing pro-apoptotic factors (e.g. cytochrome C) (Li et al., 1999; Wolff et al., 2008). The mitochondria-mediated apoptotic mechanism is essential for the removal of damaged cells, but if over-activated, it may result in the death of a large number of healthy cells and compromise liver function. Sustained apoptosis can lead to loss of hepatocytes, activating hepatic stellate cells and contributing to liver fibrosis (Chakraborty et al., 2012; Wiering et al., 2023). Fibrosis alters the structure and function of the liver, which in turn leads to cirrhosis and severe liver disease. Notably, changes in mRNA expression of some genes did not always coincide with changes in protein expression, a phenomenon observed in other studies (Chen et al., 2022). Parallel changes in mRNA levels did not always accompany the protein levels in response to dietary ZnO NPs. This discrepancy can be attributed to the influence of mRNA and protein stability, including transcriptional and/or post-translational modifications (Rigault et al., 2013). Thus, hepatic injury in rare minnows caused by dietary ZnO NPs supplementation may be related to ROS-mediated oxidative stress and apoptosis.

Lipid metabolism is essential for producing energy and regulating various physiological, reproductive, and developmental processes (Dong et al., 2016). Lipid accumulation in tissues results from the balance between synthesis and degradation, which is controlled by enzyme activity and gene expression. In our study, dietary supplementation with ZnO NPs in rare minnow induced hepatic lipid peroxidation, as evidenced by the up-regulation of adipogenesis genes such as *gpat3*, *dgat1a*, and *dgat1b* mRNA, and down-regulation of *cpt1*, *tpi1* mRNA, along with increased T-CHO and TG content and ACC and FAS enzyme activities. The findings suggest that ZnO NPs can lead to liver injury in rare minnow. For adipogenesis, FAS plays a crucial role in fatty acid biosynthesis by catalyzing the final step of the process, while ACC, as the rate-limiting enzyme, regulates fatty acid synthesis in invertebrates (Lopes et al., 2021; Thampy et al., 2000). Additionally, there appears to be a synergistic interaction between FAS and ACC (Toussant et al., 1981). FAS catalyzes fatty acid synthesis using acetyl coenzyme A and malonyl coenzyme A, which ultimately synthesizes TG (Lutfi et al., 2018). Changes in TC and TG levels and ACC and FAS enzyme contents in this experiment were similar to those of Lee et al. (2014) and Chen et al. (2021) suggesting that dietary ZnO NPs have a lipid-accumulating effect on the liver of the rare minnow. Fatty acids undergo degradation via β-oxidation, with CPT1 serving as the rate-limiting enzyme in this process within the mitochondria (McClelland, 2004). Increased CPT1 activity is associated with enhanced hepatopancreatic fat metabolism. Moreover, *srebp* promoted the concentrations of lipid synthesis genes and inhibited lipid catabolism genes, increasing fatty acid synthesis in the liver. This study showed that dietary ZnO NPs decreased *cpt1* mRNA but increased *srebp* mRNA. A similar phenomenon was also found in the study by He et al. (2022). Oxidative stress triggers lipid peroxidation, leading to the breakage and denaturation of fatty acid chains, thereby interfering with lipid synthesis and metabolism (Ayala et al., 2014). This lipid damage contributes to the accumulation of abnormal lipids in hepatocytes. Oxidative stress and cellular damage induced by ZnO NPs may interfere with the overall metabolic processes within the cell, including lipid synthesis, transport and catabolism. This interference allows an imbalance in normal lipid metabolism, which increases lipid accumulation in the liver. The inhibition of fatty acid metabolism and the activation of fatty acid synthesis and steatosis caused lipid accumulation in liver tissues, leading to hepatic injury in ZnO NPs-fed rare minnow. Therefore, it is speculated that hepatic lipid deposition is closely related to lipid peroxidation.

5. Conclusion

The current research indicated that dietary ZnO NPs caused hepatotoxicity in rare minnows through ROS-mediated activation of

oxidative stress, activation of apoptosis, and inhibition of lipid peroxidation. In addition, rare minnow treated with ZnO NPs showed a decrease in body weight and HSI, and caused liver damage. Accumulation of ZnO NPs in the liver led to elevated levels of ROS, T-SOD, T-CHO and TG. Accumulation of ZnO NPs in liver tissues up-regulated the levels of genes related to antioxidant, pro-apoptotic and lipogenesis, while down-regulating genes associated with lipid catabolism.

Ethics statement

The animal study in this paper was reviewed and approved by the Ethics Committee of the Wuhan Polytechnic University in Hubei Province, China.

CRediT authorship contribution statement

Jun Liu: Writing – review & editing, Supervision, Software, Funding acquisition. **Yongfeng He:** Writing – review & editing, Resources, Conceptualization. **Jing Wan:** Methodology, Data curation. **Jingming WU:** Writing – review & editing, Resources. **Jiahuan Wang:** Software, Methodology, Data curation. **Huanhuan Li:** Writing – original draft, Visualization, Validation, Methodology, Formal analysis, Conceptualization. **Liangxia Su:** Writing – review & editing, Visualization, Validation, Software, Resources, Project administration, Methodology, Funding acquisition, Formal analysis, Data curation, Conceptualization.

Declaration of Competing Interest

The authors declare that they have no known competing financial interests or personal relationships that could have appeared to influence the work reported in this paper.

Data Availability

Data will be made available on request.

Acknowledgements

This work was supported by the Natural Science Foundation of Hubei Province (2024AFB313), the Key Lab of Freshwater Biodiversity Conservation Ministry of Agriculture and Rural Affairs of China (2022-kj-2213), the Hubei Key Laboratory of Animal Nutrition and Feed Science (wuhan polytechnic university) (202318) and the Launching Research Fund from Wuhan Polytechnic University (53210052179).

Appendix A. Supporting information

Supplementary data associated with this article can be found in the online version at doi:10.1016/j.aqrep.2024.102317.

References

Alkaladi, A., El-Deen, N., Afifi, M., Abu Zinadah, O.A., 2015. Hematological and biochemical investigations on the effect of vitamin E and C on *Oreochromis niloticus* exposed to zinc oxide nanoparticles. Saudi. J. Biol. Sci. 22 (5), 556–563. https://doi.org/10.1016/j.sjbs.2015.02.012.

Almansour, M., Alarifi, S., Melhim, W., Jarrar, B.M., 2019. Nephron ultrastructural alterations induced by zinc oxide nanoparticles: an electron microscopic study. Iet Nanobiotechnology 13 (5), 515–521. https://doi.org/10.1049/iet-nbt.2018.5219.

Ayala, A., Muñoz, M.F., Argüelles, S., 2014. Lipid peroxidation: production, metabolism, and signaling mechanisms of malondialdehyde and 4-hydroxy-2-nonenal, 31, Article Oxid. Med. Cell. Longev. 2014, 360438. https://doi.org/10.1155/2014/360438.

Bernet, D., Schmidt, H., Meier, W., Burkhardt-Holm, P., Wahli, T., 1999. Histopathology in fish: proposal for a protocol to assess aquatic pollution. J. Fish. Dis. 22 (1) https://doi.org/10.1046/j.1365-2761.1999.00134.x.

Bordin, E.R., Ramsdorf, W.A., Domingos, L.M.L., Miranda, L.P.D., Mattoso, N.P., Cestari, M.M., 2024. Ecotoxicological effects of zinc oxide nanoparticles (ZnO-NPs) on aquatic organisms: current research and emerging trends, 15, Article J. Environ. Manag. 349, 119396. https://doi.org/10.1016/j.jenvman.2023.119396.

Chakraborty, J.B., Oakley, F., Walsh, M.J., 2012. Mechanisms and biomarkers of apoptosis in liver disease and fibrosis. Int J. Hepatol. 2012, 648915 https://doi.org/10.1155/2012/648915.

Chen, A.J., Feng, X.L., Sun, T., Zhang, Y.L., An, S.L., Shao, L.Q., 2016. Evaluation of the effect of time on the distribution of zinc oxide nanoparticles in tissues of rats and mice: a systematic review. Iet Nanobiotechnol. 10 (3), 97–106. https://doi.org/10.1049/iet-nbt.2015.0006.

Chen, S.W., Lv, W.H., Wu, K., Chen, G.H., Chen, F., Song, C.C., Luo, Z., 2021. Dietary nano-ZnO is absorbed via endocytosis and zip pathways, upregulates lipogenesis, and induces lipotoxicity in the intestine of yellow catfish. Int J. Mol. Sci. 22 (21) https://doi.org/10.3390/ijms222112047.

Chen, G.H., Song, C.C., Zhao, T., Hogstrand, C., Wei, X.L., Lv, W.H., Song, Y.F., Luo, Z., 2022. Mitochondria-dependent oxidative stress mediates ZnO nanoparticle (ZnO NP)-induced mitophagy and lipotoxicity in freshwater teleost fish. Environ. Sci. Technol. 56 (4), 2407–2420. https://doi.org/10.1021/acs.est.1c07198.

Chen, Y.J., Wu, F.X., Li, W.Y., Luan, T.G., Lin, L., 2017. Comparison on the effects of water-borne and dietary-borne accumulated ZnO nanoparticles on *Daphnia magna*. Chemosphere 189, 94–103. https://doi.org/10.1016/j.chemosphere.2017.08.132.

Choi, J.S., Kim, R.O., Yoon, S., Kim, W.K., 2016. Developmental toxicity of zinc oxide nanoparticles to zebrafish (*Danio rerio*): a transcriptomic analysis, 15, Article Plos One 11 (8), e0160763. https://doi.org/10.1371/journal.pone.0160763.

Chong, C.L., Fang, C.M., Pung, S.Y., Ong, C.E., Pung, Y.F., Kong, C., Pan, Y., 2021. Current updates on the in vivo assessment of zinc oxide nanoparticles toxicity using animal models. BioNanoScience.

Daei, S., Abbasalipourkabir, R., Khajvand-Abedini, M., Ziamajidi, N., 2023. The alleviative efficacy of vitamins A, C, and E against zinc oxide nanoparticles-induced hepatic damage by reducing apoptosis in rats. Biol. Trace Elem. Res. 201 (3), 1252–1260. https://doi.org/10.1007/s12011-022-03218-2.

De Souza, J.M., Mendes, B.D., Guimaraes, A.T.B., Rodrigues, A.S.D., Chagas, T.Q., Rocha, T.L., Malafaia, G., 2018. Zinc oxide nanoparticles in predicted environmentally relevant concentrations leading to behavioral impairments in male swiss mice. Sci. Total Environ. 613, 653–662. https://doi.org/10.1016/j.scitotenv.2017.09.051.

Dong, T.Y., Kang, X.M., Liu, Z.L., Zhao, S., Ma, W.J., Xuan, Q.J., Liu, H., Wang, Z.P., Zhang, Q.Y., 2016. Altered glycometabolism affects both clinical features and prognosis of triple-negative and neoadjuvant chemotherapy-treated breast cancer. Tumor Biol. 37 (6), 8159–8168. https://doi.org/10.1007/s13277-015-4729-8.

Faiz, H., Zuberi, A., Nazir, S., Rauf, M., Younus, N., 2015. Zinc oxide, zinc sulfate and zinc oxide nanoparticles as source of dietary zinc: comparative effects on growth and hematological indices of juvenile grass carp (*Ctenopharyngodon idella*). Int. J. Agric. Biol. 17 (3), 568–574. https://doi.org/10.17957/ijab/17.3.14.446.

Farag, M.R., Alagawany, M., Alsulami, L.S., Di Cerbo, A., Attia, Y., 2023. Ameliorative effects of *Dunaliella salina* microalgae on nanoparticle (ZnO NPs)-induced toxicity in fish. Environ. Sci. Pollut. Res., 14. https://doi.org/10.1007/s11356-023-30933-7.

Fonseca, E., Vázquez, M., Rodriguez-Lorenzo, L., Mallo, N., Pinheiro, I., Sousa, M.L., Cabaleiro, S., Quarato, M., Spuch-Calvar, M., Correa-Duarte, M.A., López-Mayán, J. J., Mackey, M., Moreda, A., Vasconcelos, V., Espiña, B., Campos, A., Araújo, M.J., 2023. Getting fat and stressed: effects of dietary intake of titanium dioxide nanoparticles in the liver of turbot *Scophthalmus maximus*, 15, Article J. Hazard. Mater. 458, 131915. https://doi.org/10.1016/j.jhazmat.2023.131915.

Fujihara, J., Nishimoto, N., 2023. Review of zinc oxide nanoparticles: toxicokinetics, tissue distribution for various exposure routes, toxicological effects, toxicity mechanism in mammals, and an approach for toxicity reduction. Biol. Trace Elem. Res. 15 https://doi.org/10.1007/s12011-023-03644-w.

Gad, S.S., Fayez, A.M., Abdelaziz, M., Abou El-ezz, D., 2021. Amelioration of autoimmunity and inflammation by zinc oxide nanoparticles in experimental rheumatoid arthritis. Naunyn-Schmiedebergs Arch. Pharmacol. 394 (9), 1975–1981. https://doi.org/10.1007/s00210-021-02105-2.

Hao, L.H., Chen, L., Hao, J.M., Zhong, N., 2013. Bioaccumulation and sub-acute toxicity of zinc oxide nanoparticles in juvenile carp (*Cyprinus carpio*): a comparative study with its bulk counterparts. Ecotoxicol. Environ. Saf. 91, 52–60. https://doi.org/10.1016/j.ecoenv.2013.01.007.

He, M.Y., Li, X.T., Yu, L.D., Deng, S., Gu, N., Li, L., Jia, J.B., Li, B.S., 2022. Double-sided nano-ZnO: superior antibacterial properties and induced hepatotoxicity in zebrafish embryos, 14, Article Toxics 10 (3), 144. https://doi.org/10.3390/toxics10030144.

Izquierdo, M.S., Ghrab, W., Roo, J., Hamre, K., Hernández-Cruz, C.M., Bernardini, G., Terova, G., Saleh, R., 2017. Organic, inorganic and nanoparticles of Se, Zn and Mn in early weaning diets for gilthead seabream (*Sparus aurata*; Linnaeus, 1758). Aquac. Res. 48 (6), 2852–2867. https://doi.org/10.1111/are.13119.

Kaya, H., Aydin, F., Gürkan, M., Yilmaz, S., Ates, M., Demir, V., Arslan, Z., 2015. Effects of zinc oxide nanoparticles on bioaccumulation and oxidative stress in different organs of tilapia (*Oreochromis niloticus*). Environ. Toxicol. Pharmacol. 40 (3), 936–947. https://doi.org/10.1016/j.etap.2015.10.001.

Lee, J.W., Kim, J.E., Shin, Y.J., Ryu, J.S., Eom, I.C., Lee, J.S., Kim, Y., Kim, P.J., Choi, K. H., Lee, B.C., 2014. Serum and ultrastructure responses of common carp (*Cyprinus carpio L.*) during long-term exposure to zinc oxide nanoparticles. Ecotoxicol. Environ. Saf. 104, 9–17. https://doi.org/10.1016/j.ecoenv.2014.01.040.

Li, P., Dietz, R., von Harsdorf, R., 1999. p53 regulates mitochondrial membrane potential through reactive oxygen species and induces cytochrome c-independent apoptosis blocked by Bcl-2. EMBO J. 18 (21), 6027–6036. https://doi.org/10.1093/emboj/18.21.6027.

Li, H., Yu, H., Zhang, X., Huang, W., Zhang, C., Wang, C., Gao, Q., Dong, S., 2023. Temperature acclimation improves high temperature tolerance of rainbow trout (*Oncorhynchus mykiss*) by improving mitochondrial quality and inhibiting apoptosis in liver. Sci. Total Environ., 169452 https://doi.org/10.1016/j.scitotenv.2023.169452.

Liu, Y., Huang, E., Xie, Y., Meng, L., Liu, D., Zhang, Z., Zhou, J., Zhang, Q., Tong, T., 2023. The effect of dietary lipid supplementation on the serum biochemistry, antioxidant responses, initial immunity, and mTOR pathway of juvenile tilapia (*Oreochromis niloticus*). Fishes 8 (11), 535 https://www.mdpi.com/2410-3888/8/11/535.

Lopes, C., Rocha, E., Pereira, I.L., Madureira, T.V., 2021. Deciphering influences of testosterone and dihydrotestosterone on lipid metabolism genes using brown trout primary hepatocytes (Article). Aquat. Toxicol. 235 (9), 105819. https://doi.org/10.1016/j.aquatox.2021.105819.

Lutfi, E., Gong, N.P., Johansson, M., Sánchez-Moya, A., Björnsson, B.T., Gutiérrez, J., Navarro, I., Capilla, E., 2018. Breeding selection of rainbow trout for high or low muscle adiposity differentially affects lipogenic capacity and lipid mobilization strategies to cope with food deprivation. Aquaculture 495, 161–171. https://doi.org/10.1016/j.aquaculture.2018.05.039.

Ma, Q. (2013). Role of nrf2 in oxidative stress and toxicity. In P. A. Insel (Ed.), Annual Review of Pharmacology and Toxicology, Vol 53, 2013 (Vol. 53, pp. 401-+). Annual Reviews. https://doi.org/10.1146/annurev-pharmtox-011112-140320.

Ma, H.B., Williams, P.L., Diamond, S.A., 2013. Ecotoxicity of manufactured ZnO nanoparticles - a review. Environ. Pollut. 172, 76–85. https://doi.org/10.1016/j.envpol.2012.08.011.

Mahjoubian, M., Naeemi, A.S., Moradi-Shoeili, Z., Tyler, C.R., Mansouri, B., 2023. Oxidative stress, genotoxic effects, and other damages caused by chronic exposure to silver nanoparticles (Ag NPs) and zinc oxide nanoparticles (ZnO NPs), and their mixtures in zebrafish (*Danio rerio)* (Article). Toxicol. Appl. Pharmacol. 472 (14), 116569. https://doi.org/10.1016/j.taap.2023.116569.

Mawed, S.A., Centoducati, G., Farag, M.R., Alagawany, M., Abou-Zeid, S.M., Elhady, W. M., El-Saadony, M.T., Di Cerbo, A., Al-Zahaby, S.A., 2022. *Dunaliella salina* Microalga Restores the metabolic equilibrium and ameliorates the hepatic inflammatory response induced by zinc oxide nanoparticles (ZnO-NPs) in male zebrafish, 22, Article Biology 11 (10), 1447. https://doi.org/10.3390/biology11101447.

McClelland, G.B., 2004. Fat to the fire: the regulation of lipid oxidation with exercise and environmental stress. Comp. Biochem. Physiol. B-Biochem. Mol. Biol. 139 (3), 443–460. https://doi.org/10.1016/j.cbpc.2004.07.003.

Mishra, P.K., Mishra, H., Ekielski, A., Talegaonkar, S., Vaidya, B., 2017. Zinc oxide nanoparticles: a promising nanomaterial for biomedical applications. Drug Discov. Today 22 (12), 1825–1834. https://doi.org/10.1016/j.drudis.2017.08.006.

Mohammady, E.Y., Soaudy, M.R., Abdel-Rahman, A., Abdel-Tawwab, M., Hassaan, M.S., 2021. Comparative effects of dietary zinc forms on performance, immunity, and oxidative stress-related gene expression in Nile tilapia, *Oreochromis niloticus* (Article). Aquaculture 532 (11), 736006. https://doi.org/10.1016/j.aquaculture.2020.736006.

Moreno-Olivas, F., Tako, E., Mahler, G.J., 2019. ZnO nanoparticles affect nutrient transport in an *in vitro* model of the small intestine. Food Chem. Toxicol. 124, 112–127. https://doi.org/10.1016/j.fct.2018.11.048.

Nayak, S.K., Panesar, P.S., Kumar, H., 2009. p53-induced apoptosis and inhibitors of p53. Curr. Med. Chem. 16 (21), 2627–2640. https://doi.org/10.2174/092986709788681976.

Nolfi-Donegan, D., Braganza, A., Shiva, S., 2020. Mitochondrial electron transport chain: oxidative phosphorylation, oxidant production, and methods of measurement (Article). Redox Biol. 37 (9), 101674. https://doi.org/10.1016/j.redox.2020.101674.

Poljsak, B., Suput, D., Milisav, I., 2013. Achieving the balance between ROS and antioxidants: when to use the synthetic antioxidants (Article). Oxid. Med. Cell. Longev. 2013 (11), 956792. https://doi.org/10.1155/2013/956792.

Pourmoradkhani, F., Moghanlou, K.S., Sohrabi, T., Imani, A., Gholizadeh, V., Anzabi, M. P., 2023. Supplementation of Siberian sturgeon (*Acipenser baerii*) diet with different zinc sources: effects on growth performance, digestive enzymes activity, hemato-biochemical parameters, antioxidant response and liver histology. Article s11259-023-10252-5 Vet. Res. Commun. 14. https://doi.org/10.1007/s11259-023-10252-5.

Rajkumar, K.S., Sivagaami, P., Ramkumar, A., Murugadas, A., Srinivasan, V., Arun, S., Kumar, P.S., Thirumurugan, R., 2022. Bio-functionalized zinc oxide nanoparticles: potential toxicity impact on freshwater fish *Cyprinus carpio*, 13, Article Chemosphere 290, 133220. https://doi.org/10.1016/j.chemosphere.2021.133220.

Reshma, V.G., Mohanan, P.V., 2017. Cellular interactions of zinc oxide nanoparticles with human embryonic kidney (HEK 293) cells. Colloids Surf. B-Biointerfaces 157, 182–190. https://doi.org/10.1016/j.colsurfb.2017.05.069.

Rigault, C., Le Borgne, F., Tazir, B., Benani, A., Demarquoy, J., 2013. A high-fat diet increases L-carnitine synthesis through a differential maturation of the Bbox1 mRNAs. Biochim. Et. Biophys. Acta-Mol. Cell Biol. Lipids 1831 (2), 370–377. https://doi.org/10.1016/j.bbalip.2012.10.007.

Rio, D.C., Ares, M., Jr, Hannon, G.J., Nilsen, T.W., 2010. Purification of RNA using TRIzol (TRI reagent) (pdb. prot). Cold Spring Harb. Protoc. 2010 (6), 5439. https://doi.org/10.1101/pdb.prot5439.

Sajadimajd, S., Khazaei, M., 2018. Oxidative stress and cancer: the role of Nrf2. Curr. Cancer Drug Targets 18 (6), 538–557. https://doi.org/10.2174/1568009617666171002144228.

Sallam, A.E., Mansour, A.T., Alsaqufi, A.S., Salem, M.E., El-Feky, M.M.M., 2020. Growth performance, anti-oxidative status, innate immunity, and ammonia stress resistance of *Siganu rivulatus* fed diet supplemented with zinc and zinc nanoparticles (Article). Aquac. Rep. 18 (10), 100410. https://doi.org/10.1016/j.aqrep.2020.100410.

Shukry, M., Albogami, S., Gewaily, M., Amer, A., Soliman, A., Alsaiad, S., El-Shehawi, A., Dawood, M., 2022. Growth performance, antioxidative capacity, and intestinal histomorphology of grey mullet (*Liza ramada*)-Fed dietary zinc nanoparticles. Biol. Trace Elem. Res. 200 (5), 2406–2415. https://doi.org/10.1007/s12011-021-02844-6.

Stoller, M., Ochando-Pulido, J.M., 2020. ZnO nano-particles production intensification by means of a spinning disk reactor, 15, Article Nanomaterials 10 (7), 1321. https://doi.org/10.3390/nano10071321.

Tang, H.Q., Xu, M., Rong, Q., Jin, R.W., Liu, Q.J., Li, Y.L., 2016. The effect of ZnO nanoparticles on liver function in rats. Int. J. Nanomed. 11, 4275–4285. https://doi.org/10.2147/ijn.S109031.

Thampy, G.K., Haas, M.J., Mooradian, A.D., 2000. Troglitazone stimulates acetyl-CoA carboxylase activity through a post-translational mechanism. Life Sci. 68 (6), 699–708. https://doi.org/10.1016/s0024-3205(00)00973-5.

Toussant, M., Wilson, M., Clarke, S., 1981. Coordinate suppression of liver acetyl-CoA carboxylase and fatty acid synthetase by polyunsaturated fat. J. Nutr. 111 (1), 146–153. https://doi.org/10.1093/jn/111.1.146.

Wang, J.W., Cao, W.X., 2017. Gobiocypris rarus as a chinese native model organism: history and current situation. Asian J. Ecotoxicol.

Wiering, L., Subramanian, P., Hammerich, L., 2023. Hepatic stellate cells: dictating outcome in nonalcoholic fatty liver disease. Cell. Mol. Gastroenterol. Hepatol. 15 (6), 1277–1292. https://doi.org/10.1016/j.jcmgh.2023.02.010.

Wolff, S., Erster, S., Palacios, G., Moll, U.M., 2008. p53's mitochondrial translocation and MOMP action is independent of Puma and Bax and severely disrupts mitochondrial membrane integrity. Cell Res. 18 (7), 733–744. https://doi.org/10.1038/cr.2008.62.

Xiao, L., Liu, C.H., Chen, X.N., Yang, Z., 2016. Zinc oxide nanoparticles induce renal toxicity through reactive oxygen species. Food Chem. Toxicol. 90, 76–83. https://doi.org/10.1016/j.fct.2016.02.002.

Xiong, D.W., Fang, T., Yu, L.P., Sima, X.F., Zhu, W.T., 2011. Effects of nano-scale TiO_2, ZnO and their bulk counterparts on zebrafish: Acute toxicity, oxidative stress and oxidative damage. Sci. Total Environ. 409 (8), 1444–1452. https://doi.org/10.1016/j.scitotenv.2011.01.015.

Yan, G.Y., Huang, Y.N., Bu, Q., Lv, L., Deng, P.C., Zhou, J.Q., Wang, Y.L., Yang, Y.Z., Liu, Q.Q., Cen, X.B., Zhao, Y.L., 2012. Zinc oxide nanoparticles cause nephrotoxicity and kidney metabolism alterations in rats. J. Environ. Sci. Health Part a-Toxic. /Hazard. Subst. Environ. Eng. 47 (4), 577–588. https://doi.org/10.1080/10934529.2012.650576.

Yao, Y., Zang, Y.T., Qu, J., Tang, M., Zhang, T., 2019. The toxicity of metallic nanoparticles on liver: the subcellular damages, mechanisms, and outcomes. Int. J. Nanomed. 14, 8787–8804. https://doi.org/10.2147/ijn.S212907.

Yudhi, N., Fina Amreta, L., Isa, N., Helbert, Firyal Nida, K., 2024. Production of reverse transcriptase from Moloney murine leukemia virus in Escherichia coli expression system. Prep. Biochem Biotechnol. (0) https://doi.org/10.1080/10826068.2024.2317311.

Zhang, Q., Xie, Y., Zhang, Y., Huang, E., Meng, L., Liu, Y., Tong, T., 2024. Effects of dietary supplementation with chitosan on the muscle composition, digestion, lipid metabolism, and stress resistance of juvenile tilapia (Oreochromis niloticus) exposed to cadmium-induced stress. Animals : Open Access J. MDPI 14 (4), 541. https://doi.org/10.3390/ani14040541.

Zheng, J.L., Luo, Z., Zhu, Q.L., Hu, W., Zhuo, M.Q., Pan, Y.X., Song, Y.F., Chen, Q.L., 2015. Different effect of dietborne and waterborne Zn exposure on lipid deposition and metabolism in juvenile yellow catfish *Pelteobagrus fulvidraco*. Aquat. Toxicol. 159, 90–98. https://doi.org/10.1016/j.aquatox.2014.12.003.

Zhu, B., Liu, L., Li, D.L., Ling, F., Wang, G.X., 2014. Developmental toxicity in rare minnow (*Gobiocypris rarus*) embryos exposed to Cu, Zn and Cd. Ecotoxicol. Environ. Saf. 104, 269–277. https://doi.org/10.1016/j.ecoenv.2014.03.018.

Zhuo, L.B., Liu, Y.M., Jiang, Y.H., Yan, Z., 2024. Zinc oxide nanoparticles induce acute lung injury via oxidative stress-mediated mitochondrial damage and NLRP3 inflammasome activation: in vitro and in vivo studies (Article). Environ. Pollut. 341 (14), 122950. https://doi.org/10.1016/j.envpol.2023.122950.